Evidence for long range movement of Bi-2212 within the filament bundle on melting and its significant effect on J_c

2011 Supercond. Sci. Technol. 24 075016

(http://iopscience.iop.org/0953-2048/24/7/075016)

Supercond. Sci. Technol. **24** (2011) 075016 (9pp) doi:10.1088/0953-2048/24/7/075016

Evidence for long range movement of Bi-2212 within the filament bundle on melting and its significant effect on J_c

A Malagoli[1], F Kametani, J Jiang, U P Trociewitz, E E Hellstrom and D C Larbalestier

Applied Superconductivity Center, National High Magnetic Field Laboratory, 2031 E Paul Dirac Drive, Tallahassee, FL 32310, USA

E-mail: malagoli@asc.magnet.fsu.edu

Received 3 February 2011, in final form 11 May 2011
Published 1 June 2011
Online at stacks.iop.org/SUST/24/075016

Abstract

It is well known that the critical current density J_c of multifilamentary Bi-2212 wires tends to decline as the wire length increases, but the reasons for and the magnitude of this decline remain obscure and quantitatively unpredictable. Here we report on the J_c and mass density variation with length on ~1 m long samples taken from two recent and representative wires, in which we find a strong decrease of J_c with distance from the end and a strong correlation between J_c and the local mass density. The mass density variations occur on length scales of centimeters, many times the nominal 15 μm filament diameter. The cause of the mass density variation appears to be internal gas pressure that generates bubbles which almost fill the filament diameter when the Bi-2212 melts. Control of this internal pressure seems to be vital to moderating or avoiding the length dependence of J_c.

1. Introduction

In large scale applications of superconductivity, research and technology development are strongly focused on material optimizations on conductor forms which can satisfy high magnetic field applications, which are widespread in physics, chemistry and biology research, for example accelerator dipoles and NMR magnets. Although the Nb-based superconductors currently dominate high field applications, it is well known that their use is limited to magnetic fields of ~18 T in saddle magnets and ~24 T in solenoids [1]. In this scenario round wires made of multifilamentary $Bi_2Sr_2CaCu_2O_x$ (Bi-2212) could make a good alternative conductor for high field magnet applications [2, 3]. Like other HTS conductors such as YBCO ($YBa_2Cu_3O_{7-\delta}$) or Bi-2223 ($(Bi, Pb)_2Sr_2Ca_2Cu_3O_x$), their higher critical temperatures may allow their use in cryogen-free systems above 4 K. Bi-2212 can maintain a J_c of about 10^5 A cm^{-2} at 4.2 K in fields above 20 T, even up to 45 T [4, 5]. Moreover, unlike YBCO and Bi-2223, which have to be processed as flat tapes to develop high J_c, it has the great technological advantage of developing high J_c in a round shape, which makes it anisotropy free and facilitates magnet design. This very useful property comes from its very particular fabrication and heat treatment process. The multifilamentary architecture is achieved by applying the typical powder-in-tube (PIT) process, filling Ag tubes with nominally phase-pure Bi-2212 powder, co-drawing them to smaller size, and applying a restacking step in many cases. At the final size the relative density of the powder in the filaments is of order 70% [6]; however, the 2212 phase is disconnected electrically. Connecting the 2212 powder particles and thus developing high J_c occurs by briefly melting the 2212 powder filaments inside the Ag sheath, then renucleating the 2212 phase on cooling. The feasibility of long length Bi-2212 wire production has already been demonstrated [7], as well as the capability of assembling such wires into Rutherford cables [8, 9]. A major challenge at this point is to make the application of Bi-2212 conductor in high field technology more compelling by increasing its critical current density J_c.

A significant issue in applying Bi-2212 to magnets is that the J_c of wires of long lengths is substantially smaller (30–50%) than in short samples [10–12]. Many studies have been made with the aim of understanding and improving the transport properties, most by studying the partial-melt

[1] Permanent address: CNR-SPIN, C.so Perrone 24, I-16152 Genova, Italy.

Table 1. Sample parameters.

Wire	Number of filaments	Powder	External diameter (mm)
W10	$85 \times 18 = 1530$	Nexans standard	1.2
W8	$37 \times 18 = 666$	Nexans granulate	0.8

process [13–16] with the goal of increasing J_c in short Bi-2212 wire samples. From such studies it is clear that the J_c of Bi-2212 wires is limited by the connectivity of the filament pack, thus making greater understanding of what controls the connectivity important.

The fact that long samples generally have lower J_c than short samples is an important impediment to their use in applications [7, 17] and it is a matter of concern that the cause of the degradation is largely unknown. It is therefore clear that understanding what causes the J_c degradation with increasing sample length is of vital importance, because it directly bears on the performance of coils. For example, the winding current densities of Bi-2212 coil packs are of order 10^4 A cm^{-2} while those of YBCO coated conductors are 3–4 times higher [18]. In spite of this lower J_c, recently a 22.5 T Bi-2212 coil operating inside a 20 T Nb–Ti/Nb_3Sn magnet operating at 4.2 K was demonstrated [19]. It is very likely that 25 T or even higher fields will soon become accessible using round wire multifilament Bi-2212 conductors if long sample J_c values can achieve the same values as found in samples of a few centimeters length.

In this paper we describe experiments that correlate local transport and magnetization I_c measurements with the microstructure of 1 m long samples heat treated both with their ends left open and with their ends closed off. We find a strong correlation between I_c and the local wire mass density, which shows major and systematic local variations. These variations appear to be due to the presence of gas inside the not fully dense Bi-2212 filaments. During the melt step, the gas that fills the ∼30% of voids inside the filament space, and perhaps the oxygen evolved in melting of the 2212 phase, agglomerates into large 'bubbles' that almost completely fill the filaments, as is shown in detail in a separate microstructural study by Kametani *et al* [20]. We believe that such 'bubbles' move the melt phase over a significant distance and are a principal cause of the length dependence of I_c and the degraded connectivity that is the cause of lowered I_c in the present Bi-2212 round wires.

2. Experimental details

In this work multiple samples of two recent and slightly different Bi-2212 round wires made by Oxford Superconducting Technology for the VHFSMC (Very High Field Superconducting Magnet Collaboration) were examined. They were both fabricated using the powder-in-tube (PIT) method [7] in which a pure silver tube was filled with Bi-2212 precursor powder and then drawn into a hexagonal form. In the present conductor architectures 85 or 37 such filaments were restacked inside a pure Ag tube and again drawn into a hexagonal shape. Eighteen of these first-stage multifilament bundles were then

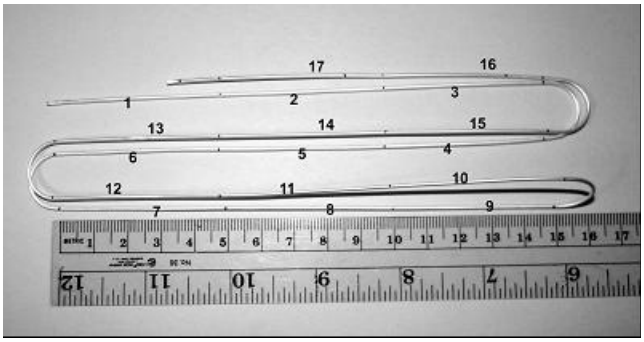

Figure 1. The serpentine sample shape used for the heat treatment of the 1 m long samples, which were then cut into 17 short samples with lengths of 5 cm. The marked number defines the position of each short sample with respect to the whole sample length.

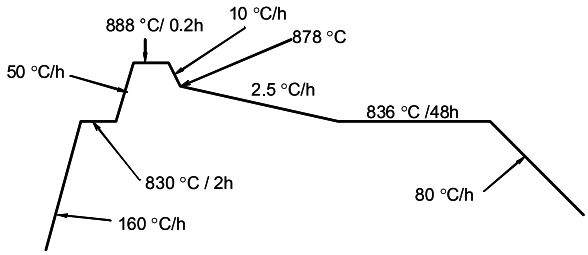

Figure 2. The heat treatment schedule used for the partial-melt process [7].

restacked in a Ag 0.2 wt% Mg alloy tube and drawn either to 0.8 mm (W8) or to 1.2 mm (W10) diameter. Table 1 gives some of the important parameters of the wires. Two different Bi-2212 precursor powders were used, both made by Nexans. The two powders have the same chemical composition, but the granulate powder has a larger average particle size than the standard powder. We believe that neither the different filament count nor the different powder was decisive for the results obtained, since the filament size in both wires is almost identical and the particle size difference vanishes during the melting process.

We analyzed 1 m long samples, performing both transport and magnetic measurements on 17 short samples (5 cm long) cut out after the heat treatment. To heat treat the 1 m samples the serpentine shape shown in figure 1 was used. This geometry was chosen because it allowed the whole sample to be within the 30 cm long homogeneous (±0.5 °C) zone of our furnace and furthermore we could extract sections of straight samples, which made the transport and other measurements easier. Figure 2 shows the schedule of the heat treatment [7] for this kind of Bi-2212 conductor. It was performed in a pure oxygen atmosphere. In one set of reactions the sample ends were left open so that gas might partially escape from the winding during heat treatment, while in a second set the ends were sealed by dipping them into liquid silver. The time of this dip was a compromise between being long enough to obtain a good seal, while short enough to avoid melting of the external sheath of the wire. Figure 3 shows the resulting sealed wire ends.

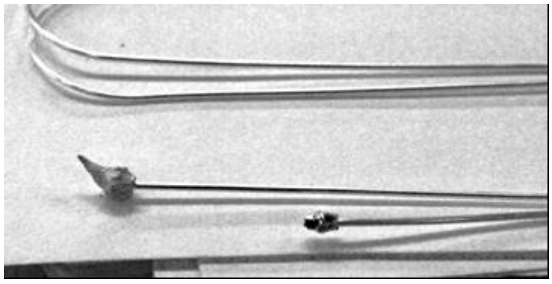

Figure 3. The sealed ends of the 1 m sample of W8. The solid silver seals resulting from dipping the wire ends into liquid silver are evident.

Critical current (I_c) transport measurements were performed in liquid helium at 4.2 K and in a magnetic background field of 5 T using the four probe method, applying an electric field criterion of 10^{-6} V cm^{-1}. The longitudinal axis of the wire was perpendicular to the field direction, while the voltage taps were located 1–1.5 cm apart in the center of the 5 cm long samples.

The hysteretic magnetization, ΔM, of short (few millimeters long) samples was measured with a 14 T Oxford vibrating sample magnetometer (VSM) at 20 K with the applied field perpendicular to the wire axis, while the critical temperature (T_c) was extracted from magnetization measurements, $m(T)$, obtained after zero-field cooling to 5 K, then heating in a field of 2 mT in a 5.5 T Quantum Design SQUID magnetometer.

For the mass density measurements, the transverse surfaces at the ends of each 5 cm sample were carefully polished until they matched a flat reference surface. Then their length was measured with a micrometer to an accuracy of 0.001 mm while their mass was measured with a balance to an accuracy of 0.01 mg. The estimated errors in the mass per unit length are 0.1% for the 0.8 mm wire and 0.08% for the 1.2 mm wire.

After the mass density and magnetization measurements, the samples were mounted in a conducting Bakelite puck and carefully polished with SiC and a final 0.05 μm alumina suspension to avoid relief and 2212 pull-out, so that the transverse cross-section could be accurately viewed. The cross-sections were imaged in an Olympus LEXT OLS3100 microscope which gave high contrast digital images with a resolution of $\sim$1 μm over the whole wire cross-section. These images were analyzed with ImageJ so as to extract the area fraction of the Ag matrix and filament packs for evaluation of the effective area of the filaments and its correlation to the mass per unit length of wires.

In order to make a secure correlation between the transport, magnetic and mass density measurements, we performed all these different analyses on the very same sample portion, which was cut from the region lying between the voltage taps of the transport I_c measurement sample.

3. Results

3.1. Open-ended samples

In figure 4 the I_c values as a function of position along the 1 m sample are shown for both W8 and W10 wires. In both wires we observed a large reduction of up to 25% in I_c with increasing distance from the end. Both wires clearly show that the highest I_c values are found at the ends of the wires. However, while the larger diameter, open-ended sample of W10 shows an irregular I_c variation, the open-ended sample of 0.8 mm diameter W8 shows more regular behavior, with I_c decreasing almost monotonically from the ends toward the center of the sample.

From measurements of ΔM at 20 K by the VSM, we estimated the irreversibility field H_{irr} by H_K, which was determined by linear extrapolation of the Kramer function $\Delta M^{0.5} H^{0.25}$ to zero. We found a quite insignificant variation of H_K with the length and therefore conclude that there is no significant variation of the pinning properties which can justify such an I_c variation. Moreover the magnetization T_c shows no significant variation along either wire, again suggesting that there is no significant length-wise variation in the quality of the 2212 phase that could explain the I_c variation.

To further address the cause of the I_c variation, we calculated the total mass per unit length of each sample cut

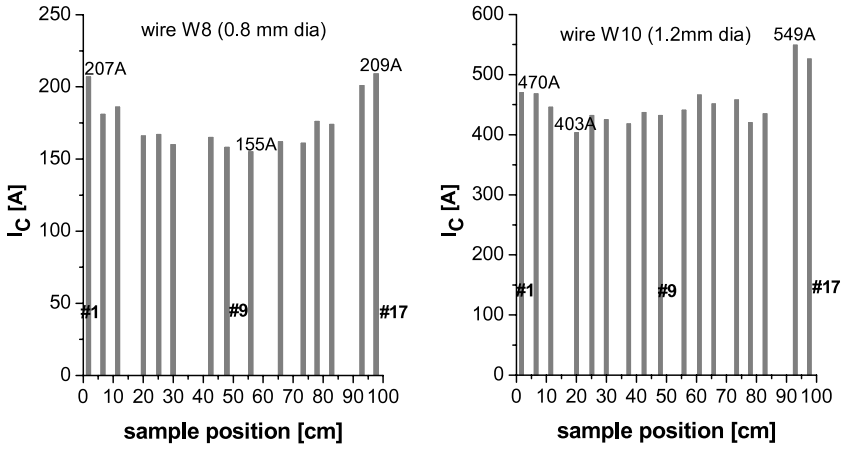

Figure 4. I_c values as a function of position in each open-ended, 1 m long W8 (left) and W10 wire length (right). The number of each sample cut from the long wires corresponds to its position in figure 1.

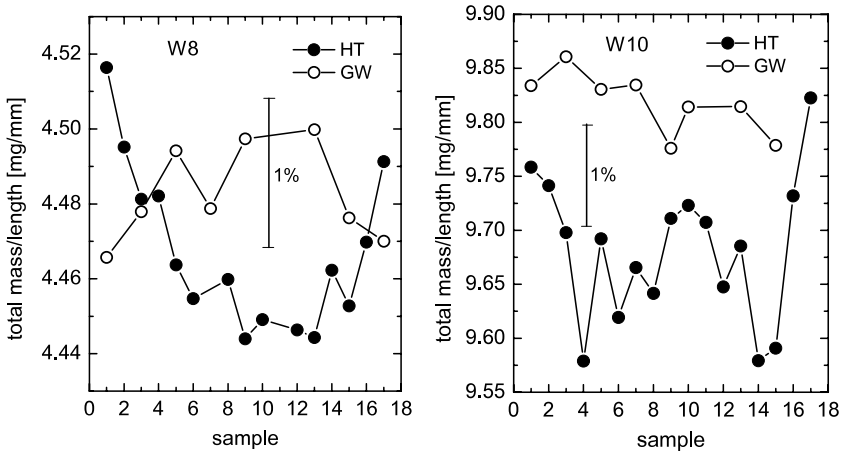

Figure 5. The total mass per unit length of each sample cut from the two open-ended reacted (HT) 1 m lengths, as well as for unreacted, 1 m 'green (GW)' samples for W8 (left) and W10 (right) wires. The x-axis defines the position number of each ∼5 cm long sample that was cut from the reacted 1 m long samples.

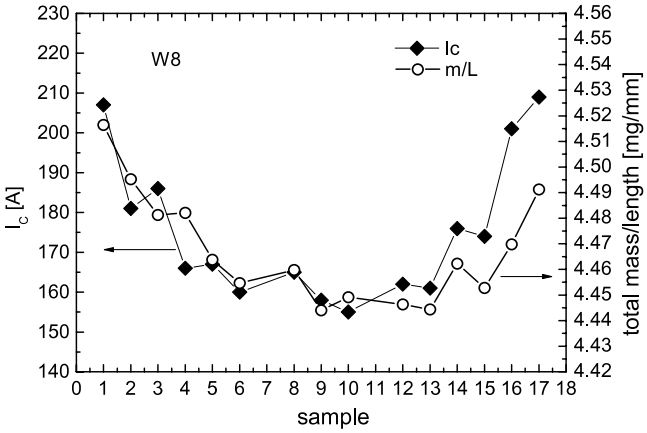

Figure 6. Comparison between the total mass per unit length and I_c for the open-ended W8 samples. The short samples #1 and #17 (which are at the ends of the 1 m sample) have the highest I_c values. An excellent qualitative correlation between mass density and I_c is evident.

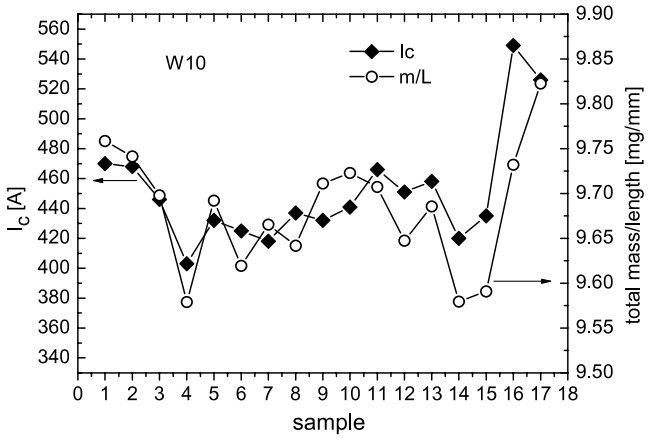

Figure 7. Comparison between the total mass per unit length and I_c for the open-ended W10 samples. As for W8, the highest I_c values are at the ends of the 1 m sample and, again, the mass density and I_c correlate well, though showing significantly more local fluctuation than in the case of W8.

from the two open-ended 1 m wires as described in section 2. Figure 5 compares these results to those obtained on 1 m green samples (i.e. final size wires before heat treatment) of both W8 and W10.

As observed for the I_c behavior, the mass per length ratio (m/L) of each wire is highest at the ends, though the end-to-center variation in W10 is more irregular than in W8. The error of these measurements is within the size of the points in the plot. Both wires show easily measurable point-to-point mass per unit length variations, which are larger for the reacted than for the 'green' wires. For W8 we observed a maximum density variation of 1.6% in the reacted samples and of 0.8% in the green samples, while for W10 we obtained maximum variations of 2.5% and 0.9% respectively. Given the large nominal Ag volume fraction of 72% and its much larger density (10.5 versus 6.6 g cm^{-3}), the linear mass density is of course dominated by the Ag, which makes these density variations, that we think are principally associated with variations of the void to Bi-2212 ratio in the filaments, so important.

The correlation between the mass per unit length and I_c reported in figures 6 and 7 for W8 and W10 is very striking. It is evident that there is a strong correlation between the mass per unit length of the wire and I_c, and even more striking that an I_c variation of about 25% corresponds to an m/L variation of only 2.5%. As noted above, we here report only the mass of the whole wire, which is a combination of the superconducting phase and the silver sheath.

The nominal filament fill factors of the two wires are 28 vol% with the filaments having a nominal void space of about 30%. Thus 2212 is nominally actually only of order 20 vol% of the total cross-section. More accurate quantifications of the real filament density and area fraction are in progress.

By quantitative image analysis of the carefully polished samples, we were able to measure the silver fraction of the transverse cross-sections of each numbered wire section and thus to evaluate the effective area of the filaments, which contain Bi-2212, other phases and porosity. In figures 8

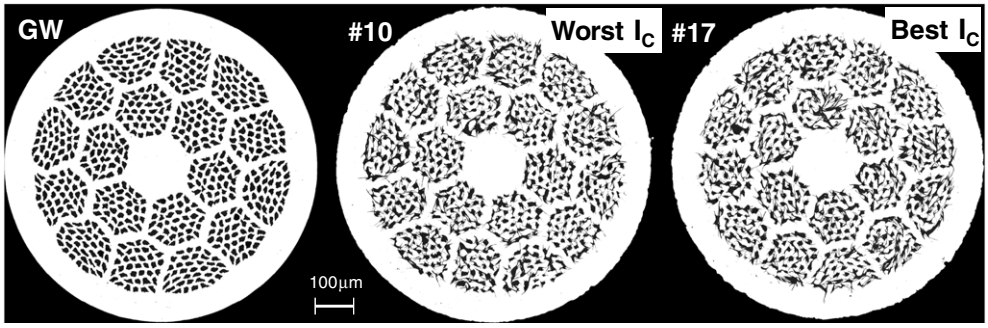

Figure 8. Cross-sections of the unreacted and two contrasting 5 cm long heat treated samples cut from the 1 m long, open-ended W8 wire.

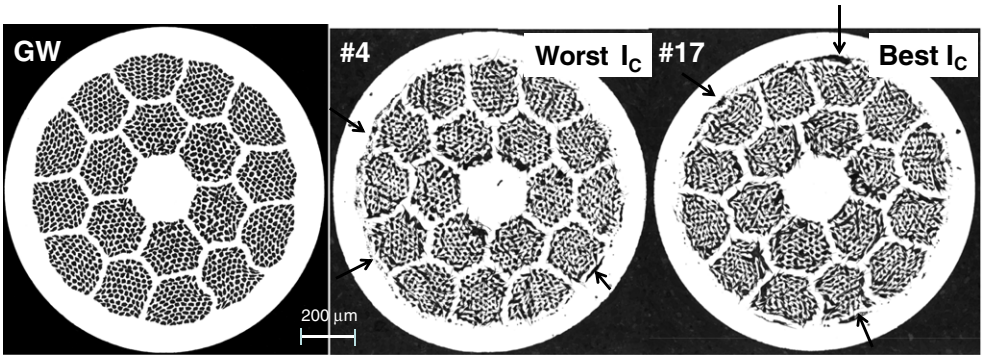

Figure 9. Cross-sections of the unreacted and two contrasting 5 cm sections of the open-ended, 1 m long heat treated W10 wire. Unlike W8, porosity in W10 also appears (as indicated by the arrows) at the interface between the filament bundles and the external sheath.

and 9 the cross-sections of the 'green wire' sample (GW) and examples of the lowest and highest I_c samples are shown for each wire.

Unlike W8, a delamination porosity in W10 also appears at the interface between the filament bundles and the external sheath. In spite of the large difference in I_c between individual samples of both W8 and W10, it seems that there is no evident difference between them in terms of the defects visible in these cross-sections. This is undoubtedly due to difficulties in avoiding either fill in of filaments by loose polishing debris or its antithesis, pull-out of the Bi-2212, especially where the mass density is locally low. A parallel study by Kametani *et al* [20] uses quenched samples and x-ray tomography to present a more detailed understanding of the nature of the voids appearing in the filaments after HT.

The measurement of the Ag area (the white fraction of the images) for each sample was made by image analysis and this allowed the calculation of the black area, which is either Bi-2212 or void. Starting from these values and knowing the total mass of the samples and the theoretical value of the Ag mass density (10.49 g cm^{-3}) we calculated the mass density of the Bi-2212 for every sample. However, the reliability of such values can be affected by uncertainty about the value of the Ag mass density after heat treatment. We therefore focused our attention on the relative variation of the Bi-2212 mass density instead of its absolute value.

In figures 10 (W8) and 11 (W10) a comparison between the behavior of I_c and the relative Bi-2212 mass density as a function of the position along the 1 m sample is shown. To compare just their length variations, both I_c and the Bi-2212 mass density have been normalized to the respective value of sample #1.

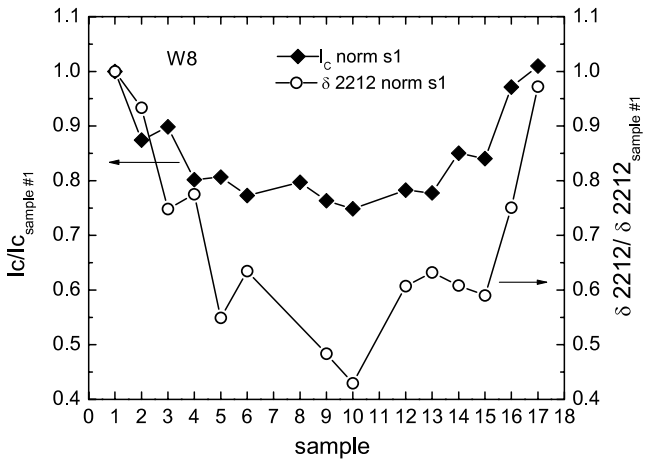

Figure 10. Comparison between the normalized I_c and the relative Bi-2212 mass density determined from image analysis of the Ag cross-section as a function of the position along the open-ended 1 m long W8 sample.

There is an evident correlation between the I_c and the Bi-2212 mass density, but it is also striking that the derived mass density variations are very large. For W8 the relative

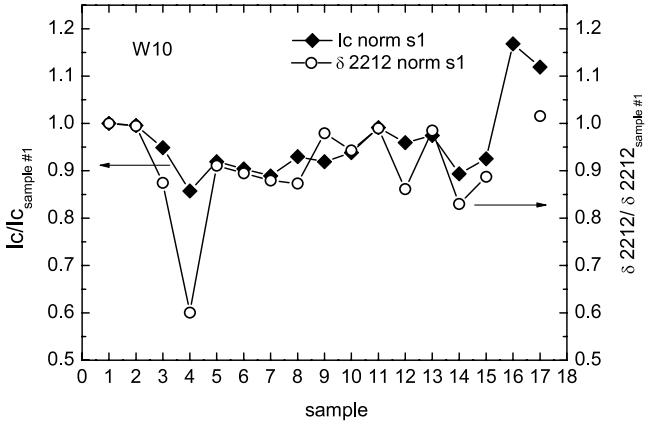

Figure 11. Comparison between the I_c and the relative Bi-2212 mass density determined from image analysis of the Ag cross-section as a function of the position along the open-ended 1 m long W10 sample.

Bi-2212 mass density fell quite smoothly to a minimum of about 45% of the maximum density near the middle of the 1 m long wire and indeed this correlated well to the minimum I_c. However, there is not a linear relation between I_c and the 2212 density since I_c declines only by about 25% while the relative density has fallen to ∼50% at this value. W10 shows somewhat different behavior. The 2212 mass density is for almost all samples directly correlated to I_c. Higher magnification images of the filaments neighboring the sheath–filament pack porosity seen, for example, in samples 4 and 17 showed considerable densification of the filament pack, perhaps the cause of the higher J_c in W10 as opposed to W8.

3.2. Studies of sealed-end samples

Because coils use many hundreds of meters of conductor, it seems plausible to imagine that any gas pressure is fully confined within the wire, unless there is a blowout that allows leakage of Bi-2212, which undoubtedly does occur on occasion [12, 21]. To see what could happen in longer wires, two additional 1 m samples of W8 and W10 were heat treated with sealed ends, as shown in figure 3, so as to inhibit relief of gas pressure through the ends. Figure 12 shows images of the W8 sample taken soon after the heat treatment of figure 2. Many Bi-2212 leaks appeared along the whole length of the wire, as is clearly evident by the black stains left on the alumina support paper used during heat treatment. Furthermore, in the magnified image, it is possible to see deep cracks in the Ag alloy sheath. To determine at what stage in the heat treatment the leakage occurred, a second closed-end W8 1 m long sample was prepared and heat treated using the same heating profile shown in figure 2 up to a maximum temperature of 870 °C—i.e. below the melting temperature of the Bi-2212—and then directly cooled down to room temperature at a constant rate of 80 °C h^{-1}.

No sign of any leak or crack of the sheath alloy was seen. This same sample then underwent the usual Bi-2212 melt process described in figure 2 with a maximum temperature of 888 °C to ensure the formation of the melt phase. The leakage

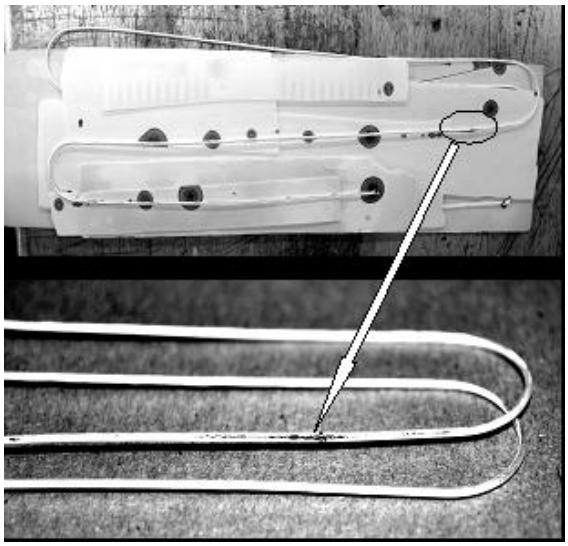

Figure 12. Images of the closed-end 1 m sample of W8 after the heat treatment shown in figure 2. In the upper picture many black stains are visible along the whole sample, indicating several sites of Bi-2212 leakage. In the lower picture a magnified view shows details of cracks in the silver sheath. No such leakage was seen in the open-ended samples.

Figure 13. Sealed W10 1 m sample after the heat treatment. Bi-2212 leakages are present only at the ends, as highlighted by the black stains on the alumina paper.

and cracking were then qualitatively identical to what is visible in figure 12. It thus seems clear that the melt step triggers the leakage.

Figure 13 presents two similar images of the sealed-end W10 wire after heat treatment. In marked contrast to W8, Bi-2212 leaks are present only at the ends and no cracks were found along the sample. This different behavior of W10 with respect to the W8 wire is probably due to the fact that the W10 has a larger outer diameter and a thicker external sheath. In this case it was possible to measure I_c as a function of the distance from the end only for W10. Figure 14 compares the results obtained on the closed- and open-end samples. The closed-end samples have uniformly lower I_c and do not show any enhancement of I_c at the ends.

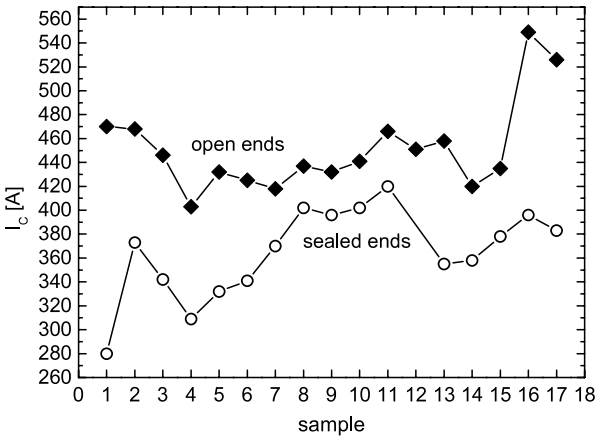

Figure 14. Comparison of the I_c values of the W10 samples with open and closed ends.

4. Discussion

The present work was undertaken as part of a broader study of the effect of different parts of the complex Bi-2212 heat treatment on the development of microstructure and J_c [13, 14]. This part of the study was incited by a concern about the effect of the residual porosity that is intrinsic to all powder-in-tube fabrication processes. To successfully deform brittle powders in a ductile matrix, the powder must be less than 100% dense, because the powder particles must break, roll or slide over each other in order to co-reduce equally with the surrounding metal. It is clear that the tap densities of 2212 in the tubes can be as little as 25–30% judging by an earlier study of Karuna *et al* [6]. However, wire drawing can densify the powder rather quickly to a terminal density of about 65–70% and rolling can enhance the density by another 5–10%, though with a tendency to saturate due to cracking of the increasingly dense cores [22]. Thus the fractional density of the filament pack before heat treatment is probably no greater than 70%. Clearly the pore space will be filled with gas, generally air, unless special arrangements to fill it with other gases like pure oxygen are made. On heating, this gas expands of the order of four times and, in addition, oxygen is emitted on the melting of the 2212 which must be picked up on subsequent cooling. An essential property of the Ag sheath and a motivation for choosing it as the sheath alloy material is that it can transmit O_2 freely, but this is not true for nitrogen or for CO_2 produced by decomposition of carbonaceous impurities in the powder or left behind on the Ag surfaces. For all of these reasons, therefore, concern about the effect of heating on the gas pressure within Bi-2212 wires is reasonable. An earlier study of what happens on heat treatment was made by Polak *et al* [23], who found that one reason for I_c or J_c to be sharply dependent on T_{max} was because the mass density of the final state Bi-2212 phase declined sharply as T_{max} increased. The decline in mass density in those studies of monofilament wires was also supported by an increased normal state resistivity and a decreased indentation hardness. It was also surmised that the density variation was produced by evolution of O_2 during melting of the Bi-2212 at T_{max} because the range of T_{max} over which the properties varied strongly was only 5–6 °C. Taken together, the above two studies show that the filament density can depend on both fabrication and heat treatment variables. Following a detailed study of the local variation of the I_c in 10 and 20 layer coils made from about 50 and 130 m of wire, Myers *et al* concluded that there was only a small variation of I_c in the samples extracted from the coil [12]. However, the I_c values of the coils were always 30–40% lower than the I_c values of representative short samples of a few centimeters length. The purpose of the present work thus was to explore the length dependence of I_c in the range where there is abundant evidence from multiple groups [2, 10, 11] that I_c is lower in samples of 1 to a few meters length as compared to samples of a few centimeters length.

Reviewing the principal results of this work, we have observed large I_c variations on several 1 m long samples taken from two different Bi-2212 round wires. We also clearly observed significant movement of the Bi-2212 inside the wires and measured a much larger length-wise density variation in heat treated, as opposed to as-drawn, green-state wires, which clearly indicates that significant movement of the Bi-2212 occurs within the filaments during the heat treatment. Comparing the sealed-end to the open-ended samples in figures 12 and 13, we can see that cracks and leaks appeared after the heat treatment in the closed-end wires but not in the open-ended samples. These cracks are a consequence of pressure inside the wires that is enhanced after sealing the ends. After relief of the pressure by sheath fracture, I_c is significantly lowered, as figure 14 shows. Furthermore, from the results obtained from the sealed-end W8 1 m sample, leaks appeared only after melting the Bi-2212 at 888 °C and not after heating to 870 °C. We thus conclude that the critical, high-pressure event inside the wire occurs during the melt stage of the Bi-2212. We leave further discussion of what actually occurs in the wire at melt to the report of Kametani *et al* [20], remarking only that the redistribution of Bi-2212 occurs over several centimeters, a scale many times larger than that of the filament diameter of ∼15 μm. Long range motion of this sort is of course a logical consequence of large internal pressure and significant filament porosity.

A direct correlation between local I_c and local Bi-2212 mass density was observed (see for example figure 10 for W8) but the fall in filament mass density (by up to one half) is about twice the relative fall of I_c, suggesting a complex percolation path of current through the multiply connected filament bundle.

Comparisons of W8 and W10 are instructive in various ways. Because both wires were designed to optimize J_c at different sizes, the filament count in the first stack was different, but in other respects they are very similar. However, obvious extra defects possessed by W10 (compare figures 8 and 9) were the delamination between the outer sheath and parts of the filament pack, and the quite irregular external shape of the wire cross-sections. These defects are highlighted in figure 15, where an artificial circumference has been drawn on two cross-sections just below the external diameter. These asymmetries of W10 occurred during the heat treatment and were not visible in the green sample cross-section in figure 9. We tentatively assign the cause of the 'delamination' to an

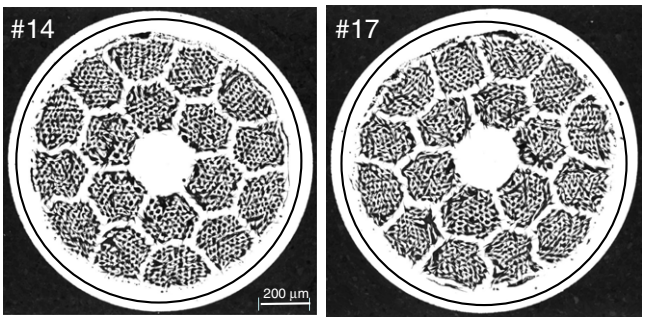

Figure 15. Cross-sections after heat treatment of two short samples taken from the open-ended 1 m long W10 sample. Porosity arising from delamination at the sheath–filament pack interface is evident, as is also an irregular outer circumference, which is not as round as in the unreacted wire. The black circles are added as a guide for the eye. They clearly show that the reacted wire can lose its initial roundness.

imperfect cleaning and perhaps to impurities in the metallic sheath. For example, some residual grease on the inner side of the external sheath could generate significant amounts of C-rich gas and cause delamination during heat treatment. The rather randomly spread defects seen in figure 15 could be the cause of the irregular variation of both I_c and the mass density in W10 samples. Just for this reason, we believe that the W8 wire is more representative of the properties of a well-built Bi-2212 round wire. Indeed, for W8, the I_c varies rather symmetrically with position from the end, as is clearly shown in figures 4 and 6.

As a confirmation of the general nature of the results observed in W8, a similar I_c behavior was reported also by Lehndorf *et al* [24] regarding a 1.2 m long Bi-2212 round multifilamentary wire, although the authors did not deeply stress this observation, since other issues were the principal topic of their work.

From the results obtained in this work it seems clear that the pressure moves the liquid Bi-2212 toward the ends of the wire during the melt stage, leading to a lower I_c in the center and a higher I_c at the ends. This new observation has significant implications for applications. The first is the obvious one that management and control of filament porosity and its wire-to-wire and along-wire variation is important and likely an effective and promising way to raise J_c. The second is the recognition that most short sample measurements in the literature will have been compromised by uncertain effects provided by the bubbling that occurs on melting. Work is already in progress on how to better define more reproducible conditions for short and long sample measurements.

5. Conclusions

We reported on the variation of I_c along 1 m long samples taken from two similar Bi-2212 wires. Magnetization evaluations of both T_c and the irreversibility field H_{irr} showed no change in quality of the Bi-2212 phase with length, even though I_c fell strongly as the distance from the end of the wire increased. The transport I_c variation was directly correlated to the variation of mass density of the wires, in which movement of Bi-2212 inside the wire during heat treatment was clearly demonstrated. The comparison between the effects of the heat treatment on samples with open ends and sealed ends showed that such Bi-2212 movement is caused by internal pressure generated during the Bi-2212 melt stage. Furthermore, we showed a strong variation of wire mass per unit length with distance from the ends and a direct correlation to the variation of I_c. Considering that we observed a Bi-2212 mass density variation on a scale of centimeters, many times larger than the $\sim$15 μm filament diameter, it is reasonable to think that the internal gas pressure produces long range motion of the liquid, leading to quite an inhomogeneous distribution of the liquid from which the Bi-2212 phase forms on later cooling. Control of this internal pressure is therefore vital not only to improve the grain connectivity and the critical current density, but also so as to moderate or avoid the length dependence of J_c which significantly degrades the expected performance of coils at the present time.

Acknowledgments

We are very grateful for discussions with all members of the HTS R&D group at ASC, especially M Dalban-Canassy, D Myers and T Shen, to V Griffin and N Craig for technical support, and for discussions within VHFSMC, especially with A Ghosh of BNL. Discussions with Y Huang and H Miao at OST are also gratefully acknowledged. The work was supported by the Very High Field Superconducting Magnet Collaboration, an ARRA grant of the US Department of Energy and by the National High Magnetic Field Laboratory which is supported by the National Science Foundation under NSF/DMR-0084173 and by the State of Florida.

References

[1] Bhattacharya A 2010 *Nature* **463** 605
[2] Godeke A, Cheng D W, Dietderich D R, Hannaford C R, Prestemom S O, Sabbi G, Wang X R, Hikichi Y, Nishioka J and Hasegawa T 2009 *IEEE Trans. Appl. Supercond.* **19** 2228
[3] Weijers H W, Trociewitz U P, Marken K, Meinesz M, Miao H and Schwartz J 2004 *Supercond. Sci. Technol.* **17** 636
[4] Miao H, Marken K R, Meinesz M, Czabaj B and Hong S 2005 *IEEE Trans. Appl. Supercond.* **15** 2554
[5] Trociewitz U P, Schwartz J, Marken K, Miao H, Meinesz M and Czabaj B 2005 Bi2212 superconductors in high field applications *National High Magnetic Field Laboratory Research Report*
[6] Karuna M, Parrel J A and Larbalestier D 1995 *IEEE Trans. Appl. Supercond.* **5** 1279
[7] Marken K R, Miao H, Meinesz M, Czabaj B and Hong S 2003 *IEEE Trans. Appl. Supercond.* **13** 3335
[8] Hasegawa T *et al* 2001 *IEEE Trans. Appl. Supercond.* **11** 3034
[9] Barzi E, Turrioni D, Kikuchi A, Lamm M, Rusy A, Yamada R and Zlobin A V 2008 *Adv. Cryog. Eng.* **54** 431
[10] 2011 Oxford Superconducting Technology, private communication
[11] Ghosh A 2011 *BNL* private comunication
[12] Myers D *et al* in preparation
[13] Shen T, Jiang J, Yamamoto A, Trociewitz U P, Schwartz J, Hellstrom E E and Larbalestier D 2009 *Appl. Phys. Lett.* **95** 152516

[14] Shen T, Jiang J, Kametani F, Trociewitz U P, Larbalestier D, Schwartz J and Hellstrom E E 2010 *Supercond. Sci. Technol.* **23** 025009
[15] Koizumi T, Hasegawa T, Nishioka J, Hikichi Y, Nakatsu T, Kumakura H, Kitaguchi H, Matsumoto A and Nagaya S 2005 *IEEE Trans. Appl. Supercond.* **15** 2538
[16] Matsumoto A, Kitaguchi H, Kumakura H, Nishioka J and Hasegawa T 2004 *Supercond. Sci. Technol.* **17** 989
[17] Marken K R, Miao H, Meinesz M, Czabaj B and Hong S 2006 *IEEE Trans. Appl. Supercond.* **16** 992
[18] Weijers H W *et al* 2010 *IEEE Trans. Appl. Supercond.* **20** 576
[19] Friend C M, Miao H, Huang Y, Melhem Z, Domptail F, Meinesz M, Hong S, Young E A and Yang Y 2010 *IEEE Trans. Appl. Supercond.* **20** 583
[20] Kametani F *et al* 2011 *Supercond. Sci. Technol.* **24** 075009
[21] Godeke A *et al* 2007 *IEEE Trans. Appl. Supercond.* **17** 1149
[22] Satou M, Yamada Y, Murase S, Kitamura T and Kamisada Y 1994 *Appl. Phys. Lett.* **64** 640
[23] Polak M, Zhang W, Polyanskii A, Pasthiski A, Hellstrom E and Larbalestier D C 1997 *IEEE Trans. Appl. Supercond.* **7** 1537
[24] Lehndorff B, Piel H, Hortig M, Schulz G W and Theisejans R 1997 *IEEE Trans. Appl. Supercond.* **7** 1687